CET CHEMICAL ENGINEERING TRANSACTIONS

VOL. 126, 2026

A publication of AIDIC
The Italian Association of Chemical Engineering
Online at www.cetjournal.it

Guest Editors: Valerio Cozzani, Bruno Fabiano, Genserik Reniers

ISBN 979-12-81206-27-4; **ISSN** 2283-9216

DOI: 10.3303/CET26126029

Consequence Assessment of Detonations in Explosive Material Handling Facilities: An Integrated Approach

Cristian Giovanniello[a], Luca Fiorentini[a], Andrea Respighi[a], Valentina Busini[b,*]

[a]Tecsa s.r.l., Via Figino 101, 20016, Pero (Milan), Italy
[b]Politecnico di Milano – Department of Chemistry, Materials anche Chemical Engineering “Giulio Natta”, Piazza L. da Vinci 32, 20133, Milan, Italy
valentina.busini@polimi.it

Facilities handling explosives present severe risks where standard safety distances often fail to capture complex detonation phenomena. This work introduces an integrated framework combining Computational Fluid Dynamics to simulate blast wave propagation and a probabilistic Monte Carlo model for fragment projection. By simulating site-specific interactions and stochastic debris trajectories, this methodology overcomes the limitations of empirical models. The result is a robust, multi-vector risk assessment tool that provides accurate consequence analysis for safety and territorial planning.

1. Introduction

The industrial handling and storage of high explosives represent a specific sector within the process industry that demands rigorous safety protocols. In the European Union, these facilities constitute approximately 6 % of Seveso sites, yet historical analysis reveals a consistent pattern of severe accidents (Major Accident Hazards Bureau Security Technology Assessment Unit, 2023). Unlike typical chemical incidents, detonations often entail rapid escalation that renders active mitigation strategies ineffective, posing severe risks to emergency responders and surrounding areas. Currently, risk management in this sector relies heavily on passive protection and territorial planning based on Quantity-Distance (QD) standards, such as those outlined in U.S. DoD regulations (Department of Defense, 2024) or NATO manuals (NATO, 2023). While these empirical protocols provide a necessary baseline, they generally assume "free-field" conditions. Consequently, standard safety distances often fail to account for the complex reflection and channelling of blast waves caused by site-specific topography and protective embankments, leading to potential underestimation of the hazard footprint in complex geometries (*UFC 3-340-02,* 2005). To address these limitations, this paper introduces a novel, integrated consequence assessment framework applied to a real-world munition storage facility. Merging rapid empirical-probabilistic assessments with high-fidelity overpressure analysis, the methodology moves beyond simplified equations. Specifically, it employs Monte Carlo simulations for stochastic fragment projection alongside Viper::Blast—a specialized CFD code that provides precise shockwave modelling while significantly reducing run-times compared to traditional hydrocodes (Chester et al., 2024). Ultimately, this combined approach establishes a robust, accurate, and accessible standard for safety analysis, land-use planning, and the systematic drafting of Safety Reports.

2. Methodology: case study and source term characterization

The reference facility consists of 15 storage depots and associated processing buildings, handling a variety of energetic materials including TNT, RDX, Composition B, and propellants. The source term characterization is critical. For each depot, the total "TNT equivalent" mass (W_{TNT}) was calculated based on the specific heat of detonation of the stores substances relative to standard TNT ($H_{d,TNT} \simeq$ 4,520 kJ/kg), using thermochemical data from Meyer et al. (2002). To account for energy dissipation, specific damping coefficients were applied. As suggested by Manca (2013), a structural damping factor of 0.70 was applied to account for the energy absorbed by the depot walls and crater formation. Furthermore, for encased munitions, a coefficient of 0.60 was used to

Paper Received: 17 December 2025; Revised: 3 March 2026; Accepted: 29 April 2026
Please cite this article as: Giovanniello C., Fiorentini L., Respighi A., Busini V., 2026, Consequence Assessment of Detonations in Explosive Material Handling Facilities: An Integrated Approach, Chemical Engineering Transactions, 126, 169-174 DOI:10.3303/CET26126029

represent the energy consumed by the rupture of metallic casings, consistent with the findings of Cooper (1996) and Mendonça-Filho et al. (2008).

2.1 Blast wave modelling

Blast wave propagation was simulated using *Viper::Blast*, a CFD code optimized for the airblast environment resulting from high explosive detonations (Stirling Simulation Services Limited, 2024). The software offers six solver modules distinguished primarily by their management of computational resources; while five options utilize an ideal single-material solver, the selected module employs a multi-material approach incorporating the Jones-Wilkins-Lee (JWL) Equation of State (EoS). The use of the JWL EoS is essential to account for the expansion phase of explosive products and accurately describe the thermodynamics of detonation products in the near-field (Chester et al., 2024). A three-stage "remapping" technique was implemented to balance computational coast and accuracy:

- Phase 1 (Near-Field): High-resolution domain 35 x 50 x 50 m (0.1 m mesh) centered on the charge to capture the initial detonation and interaction with the depot structure.
- Phase 2 (Mid-Field): Expansion to a larger domain 235 x 220 x 80 m (0.4 m mesh) to propagate the shockwave through embankments and nearby buildings.
- Phase 3 (Far-Field): Full domain simulation 600 x 550 x 150 m (1 m mesh) to track wave decay down to 0.03 bar. It is worth noting that while regulatory limits vary internationally, this specific value represents the lowest threshold for indirect effects and reversible injuries according to Italian land-use planning regulations (Italian Decree 09/05/2001).

The simulation employs an Advection Upstream Splitting Method with Diffusion Velocity (AUSMDV) Finite Volume Method with MUSCL-Hancock time integration and an adaptive time-step strictly satisfying the Courant-Friedrichs-Lewy (CFL) condition. To manage computational costs, the minimum resolvable obstacle size dynamically matches the grid resolution. Consequently, fine details are captured in the near-field (0.1 m mesh), whereas the far-field (1.0 m mesh) naturally filters them out, retaining only macroscopic structures (e.g., embankments and main buildings) critical for blast wave diffraction.

2.2 Probabilistic fragment modeling

Debris projection was analyzed using a Python-based Monte Carlo simulation (10,000 iterations per scenario). The ballistic limit distance was calculated by solving the equations of motion including aerodynamic drag, as described by (van der Voort and Weerheijm, 2013), see Eq.(1) :

$$R = \frac{1}{k} \cdot \ln\left(1 + \frac{2k \cdot V_0^2 \cdot \alpha}{g}\right) \tag{1}$$

where g is the gravitational acceleration, α is the launch angle, and k is the ballistic coefficient (m^{-1}). The latter accounts for the aerodynamic properties of the debris and is defined in Eq.(2):

$$k = \frac{S_N \cdot \rho_a \cdot C_D}{2 \cdot \rho \cdot L} \tag{2}$$

where S_N is the shape number (for concrete debris, an appropriate number is 1.5), ρ_a is the air density (kg/m^3), ρ is the fragment density (2500 kg/m^3 for concrete), L is the characteristic length of the fragment (m), and C_D is the drag coefficient (dimensionless), which varies as a function of the Mach number. The initial launch velocity (v_0), which in (van der Voort and Weerheijm, 2013) is also referred to as Debris Launch Velocity (*DLV*), depends on the internal pressure generated by the explosion, as shown in Eq. (3):

$$v_0 = DLV = 525 \cdot \sqrt{\frac{W}{V^{2/3} \cdot \rho \cdot s}} \tag{3}$$

Where W is the net explosive mass (kg), V is the internal volume of the depot (m^3), and s is the wall thickness (m). Stochastic parameters were sampled from distributions based on literature:

- Fragment Size (L): Sampled to represent the characteristic length of debris (5-25 mm) (van der Voort and Weerheijm, 2013).
- Drag coefficient (C_D): sampled based on fragment velocity referencing NATO AASTP-1 data for irregular fragments ("AASTP-1 NATO GUIDELINES FOR THE STORAGE OF MILITARY AMMUNITION AND EXPLOSIVES," 2010).
- Launch angle (α): model assuming a Gaussian distribution (μ = 5°, σ = 9°). The sampling domain was truncated to the interval [0°, 23°]; this upper limit accounts for about 95% of the probability distribution,

while the lower limit is set to zero to exclude downward trajectories that would result in immediate ground impact.

Deterministic prediction of parameters like shape number, launch angle, and fragment size is highly uncertain, yet the ballistic model is extremely sensitive to them (e.g., larger fragments experience less drag and travel further). To manage this sensitivity, a Monte Carlo approach with 10,000 iterations was adopted. By sampling these variables from statistical distributions rather than assigning arbitrary values, the framework inherently absorbs individual parameter uncertainties, yielding a robust probability distribution of projection distances instead of a single unreliable estimate.

3. Results and Discussion

3.1 Blast wave propagation

The CFD results highlight the critical role of site topography. Here, only the results from three depots are presented for illustrative purposes. *Scenario A:* depot 1 contains about 809 kg of TNT equivalent. The simulation demonstrates a non-uniform pressure field (*Figure 1a*). The blast wave interacts with adjacent embankments, causing diffraction. Unlike a free-field model, the CFD solution shows pressure "shadows" and intensifications. The 0.03 bar threshold (reversible injuries) extends to 214 m, but the shape is distorted by local geometry (*Figure 1b - Figure 1c*).

a. b.

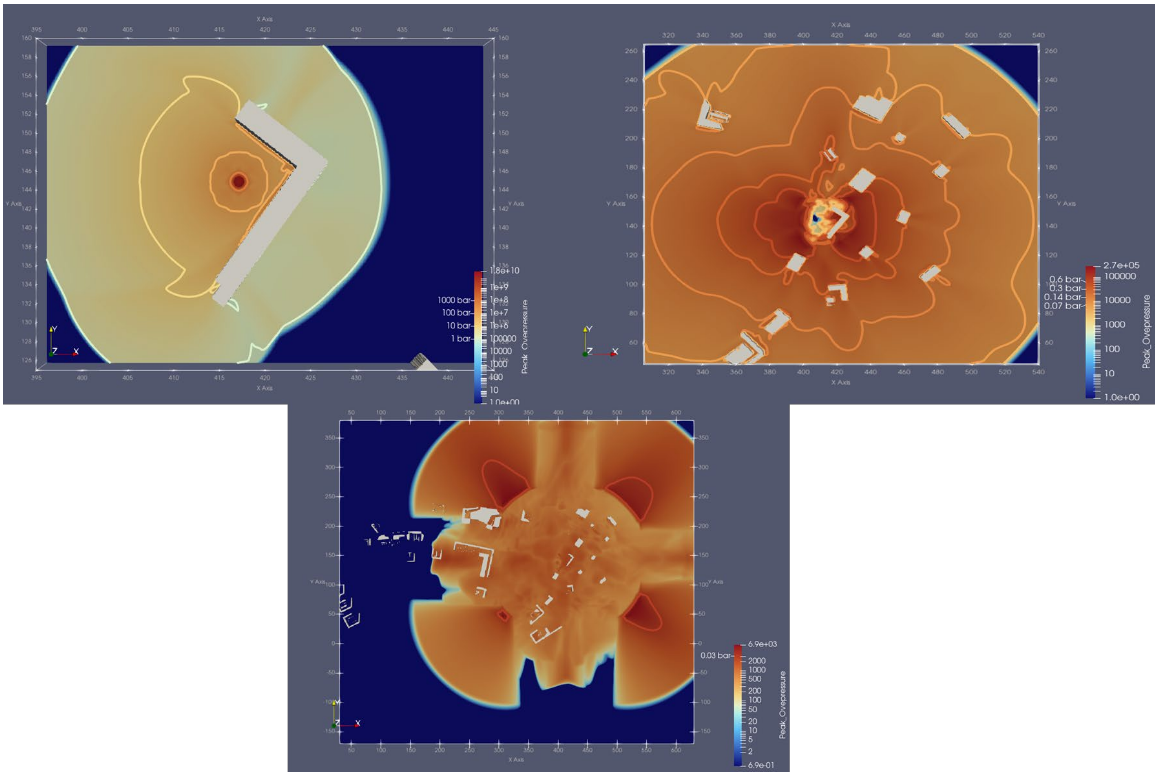

c.

Figure 1 result deposit no. 1: a. run of phase 1, b. run of phase 2, c. run of phase 3.

Scenario B: Depot 5 stores Composition B (2,778 kg TNT eq.). *Figure 2*a illustrates the results of the first calculation cycle, showing the overpressure values recorded during the initial moments of the wave evolution. In this case, higher peaks near the epicentre of approximately 10,000 bar are recorded, due to the larger quantity of explosive analysed. Such extreme magnitudes are physically realistic for the immediate near field of solid explosive detonations; as outlined in the *UFC 3-340-02, (2005)*, theoretical pressures at the detonation front can range from 180,000 to 350,000 bar before undergoing a rapid exponential decay.

*Figure 2*b reports the result at the end of the second calculation run, highlighting some of the threshold values assumed by the overpressure wave. Finally, in *Figure 2*c, the conclusive data of the third calculation run presents the last threshold value assumed by the overpressure wave (0.14 bar extends to 114 m).

a. b.

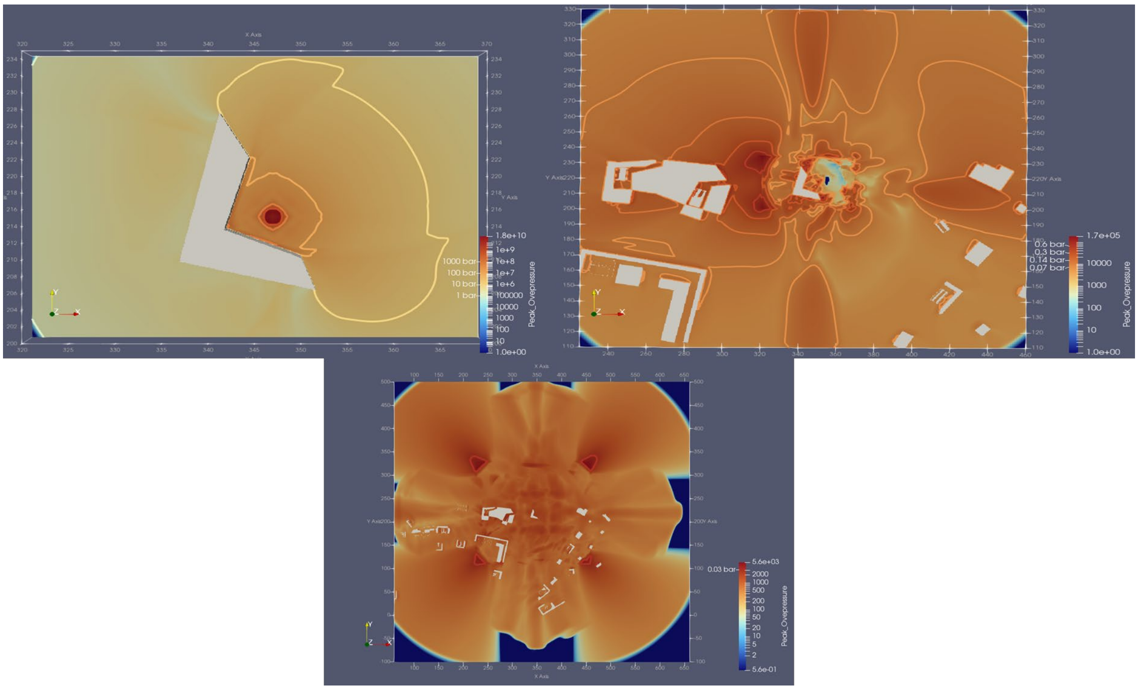

c.

Figure 2: result deposit no. 5: a. run of phase 1, b. run of phase 2, c. run of phase 3.

Scenario C: depot 10 (2,280 kg TNT eq.) presents a unique case due to its proximity to identical structures. At the end of the first calculation process, Figure 3a displays the values assumed by the overpressure wave in its initial moments. Figure 3b illustrates the result of the second calculation run, indicating some threshold values reached by the overpressure wave. Figure 3c shows the result of the third calculation run, from which the threshold values of 0.07 and 0.03 bar were extrapolated. This is the only case where an additional simulation on a larger domain was required. The result of the fourth calculation run, visible in Figure 3d, concludes the analysis showing the final threshold value encountered.

a. b.

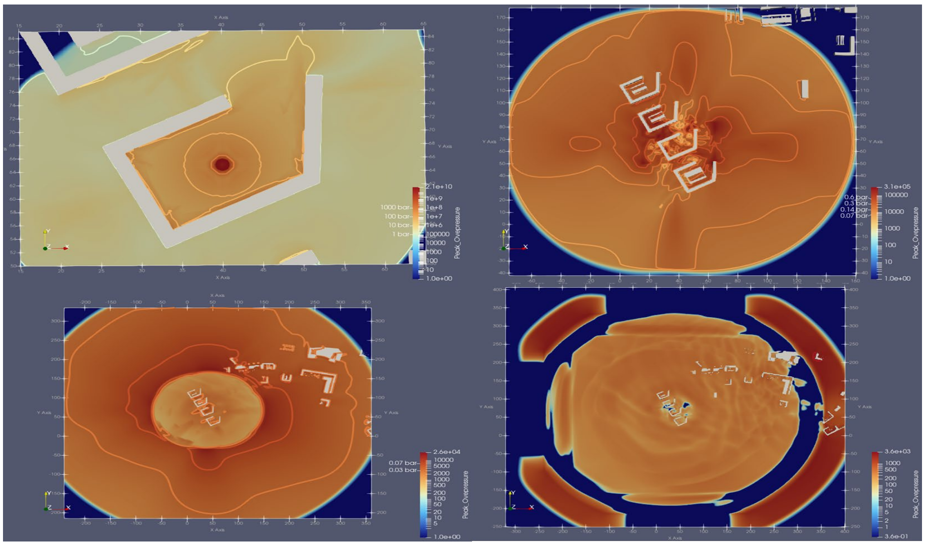

c.

Figure 3: result deposit no. 10: a. run of phase 1, b. run of phase 2, c. run of phase 3.

3.2 Analysis of fragment dispersion

The Monte Carlo simulations confirmed that fragments often dictate safety distances for lethality, consistent with DoD standards (Department of Defense, 2024). Consistent with the high explosive mass, Depot 5 generates high-velocity fragments. The histogram shows a tail extending up to 400 m. This range significantly exceeds the 114 m lethal blast radius, confirming that fragmentation is the dominant far-field hazard for open-air scenarios.

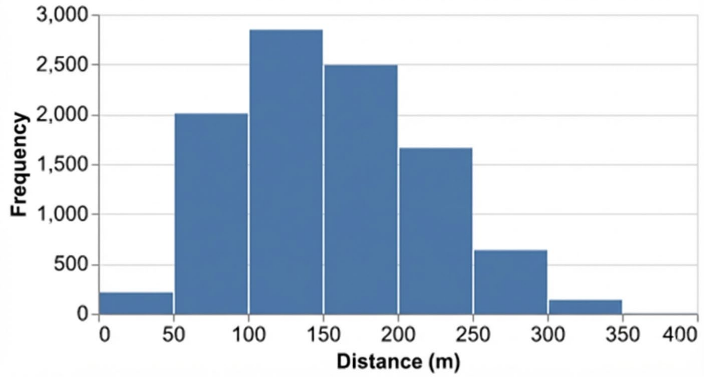

Figure 4: distance "R" of fragment fallout deposit no. 5

Depots 9 and 10 exhibit similar behaviour due to comparable explosive loads. For Depot 10 (net mass 4,500 kg), the simulation indicates a maximum range of 400 m, with most fragments landing between 50 and 250 m as shown in Graphic 2. This confirms that structural debris presents a hazard significantly beyond the blast lethality radius.

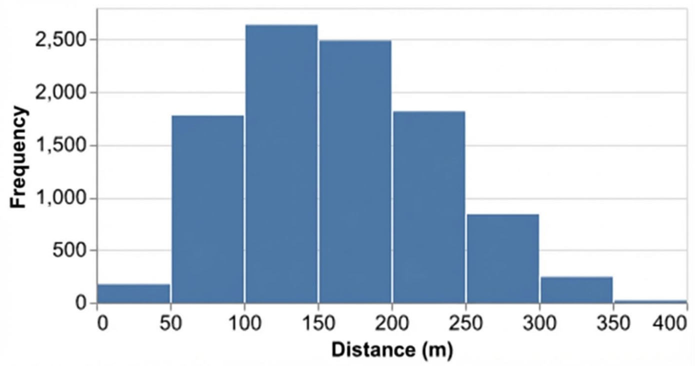

Figure 5: distance "R" of fragment fallout deposit no. 10

It is important to note that the Monte Carlo trajectory model calculates the 1D maximum radial flight distance and does not explicitly account for the 3D obstacles (e.g., embankments) defined in the CFD analysis. While embankments are primarily designed to intercept fragments with low horizontal launch angles, dedicated structural penetration tools would be required to quantify the exact stopping rate. Consequently, the probabilistic model conservatively assumes an isotropic, uniform 360-degree distribution of fragments at the calculated distances. Unlike the directional pressure maps generated by the CFD, producing a highly precise 2D/3D debris map would require fully coupled hydro-structural codes (e.g., FEM/Explicit dynamics) to model the exact physical break-up of the building and the subsequent discrete collisions with the surrounding topography.

4. Conclusions

This study demonstrates that a simulation-based approach provides a superior basis for risk assessment compared to traditional tabulated methods. While empirical formulas (e.g., Kingery-Bulmash) generally assume free-field conditions, the use of *Viper::Blast* revealed that local topography and barriers fundamentally alter blast wave propagation, creating non-symmetrical hazard zones that simplified models fail to predict. Furthermore, the probabilistic analysis confirms that secondary fragmentation is the primary driver of lethality at extended distances. When overlaid with territorial planning criteria (e.g., Italian Decree 09/05/2001), the results for this specific case study indicate potential incompatibilities between the facility hazard footprint and surrounding areas. Although compliance must be evaluated on a case-by-case basis for different sites, this level of detailed output allows for targeted mitigation strategies impossible to define using generic safety distances. Future work should extend the present analysis by including the estimation of toxic substance fallout generated by the explosion through the application of dispersion modelling.

Nomenclature

C_D - drag coefficient
G – gravitational acceleration, m/s^2
$H_{d,TNT}$ – specific heat of detonation of TNT
K – Ballistic coefficient, m^{-1}
L – fragment characteristic length, m
Q – net explosive mass, kg
R – ballistic limit distance, m
S – wall thickness, m
S_N – shape number
V – internal volume of the depot, m^3
V_0 – initial launch velocity, m/s
W_{TNT} – TNT equivalent mass, kg
α – launch angle, °
φ – material density, kg/m^3
$φ_a$ – air density, kg/m^3
-

Acknowledgments

This work originated as a Master Thesis by C. Giovanniello, who acknowledges his dual affiliation as a PhD student at Politecnico di Milano and an employee at Tecsa s.r.l. The authors allow for the technical framework provided by Tecsa s.r.l. for the development of the study.

References

AASTP-1 NATO GUIDELINES FOR THE STORAGE OF MILITARY AMMUNITION AND EXPLOSIVES, 2010. URL https://www.dau.edu/aastp-1-nato-guidelines-storage-military-ammunition-and-explosives.

Chester, A., Critchley, R., Hazael, R., 2024. A comparison of far-field explosive loads by a selection of current and emerging blast software. International Journal of Protective Structures 20414196241248192. https://doi.org/10.1177/20414196241248192

Cooper, P.W., 1996. Explosives Engineering. John Wiley & Sons.

Department of Defense, 2024. DOD 6055.9 STD - DOD AMMUNITION AND EXPLOSIVES SAFETY STANDARDS [WWW Document]. URL https://standards.globalspec.com/std/384800/dod-6055-9-std.

Major Accident Hazards Bureau Security Technology Assessment Unit, 2023. Explosives and Pyrotechnic Sites - Seveso inspection series - good practice report.

Manca, D., 2013. Quantitative assessment in safety reports of the consequences from the detonation of solid explosives. Journal of Loss Prevention in the Process Industries 26, 974–981. https://doi.org/10.1016/j.jlp.2013.10.010

Mendonça-Filho, L.G., Bastos-Netto, D., Guirardello, R., 2008. Estimating the TNT equivalence of a 15-ton single base powder explosion through damaged building profiles analyses. Journal of Hazardous Materials 158, 599–604. https://doi.org/10.1016/j.jhazmat.2008.02.004

Meyer, R., Köhler, J., Homburg, A., 2002. Explosives. Weinheim : Wiley-VCH.

NATO, 2023. NATO - AASTP-1.1 - MANUAL FOR THE DEVELOPMENT OF AN EXPLOSIVES SAFETY SITE PLAN BASED ON AASTP-1 URL https://standards.globalspec.com/std/14595454/aastp-1-1.

Stirling Simulation Services Limited, 2024. Viper::Blast.

UFC 3-340-02 Structures to Resist the Effects of Accidental Explosions, 2005.

van der Voort, M.M., Weerheijm, J., 2013. A statistical description of explosion produced debris dispersion. International Journal of Impact Engineering 59, 29–37. https://doi.org/10.1016/j.ijimpeng.2013.03.002